Supplementary Material

Wall Deposition Patterns for Nanoparticles in an Inflamed Patient-Specific Arterial Tree

Shaolie S. Hossain[a], Thomas J.R. Hughes[b], Paolo Decuzzi[a]

[a]Department of Translational Imaging and Department of Nanomedicine, The Methodist Hospital Research Institute, 6670 Bertner Avenue, Houston, TX 77030, USA
[b]Institute for Computational Engineering and Sciences, The University of Texas at Austin, 201 East 24th Street, Stop C0200, Austin, TX 78712, USA

Supplementary Figure 1: Time evolution of particle volumetric concentration at A) 1 s, B) 5.25 s, and C) 8 s. Right column plots the area-averaged quantity normalized by the number of particles injected n_{inj} and averaged over the surface area along the vessel centerline ("*Z*"direction).

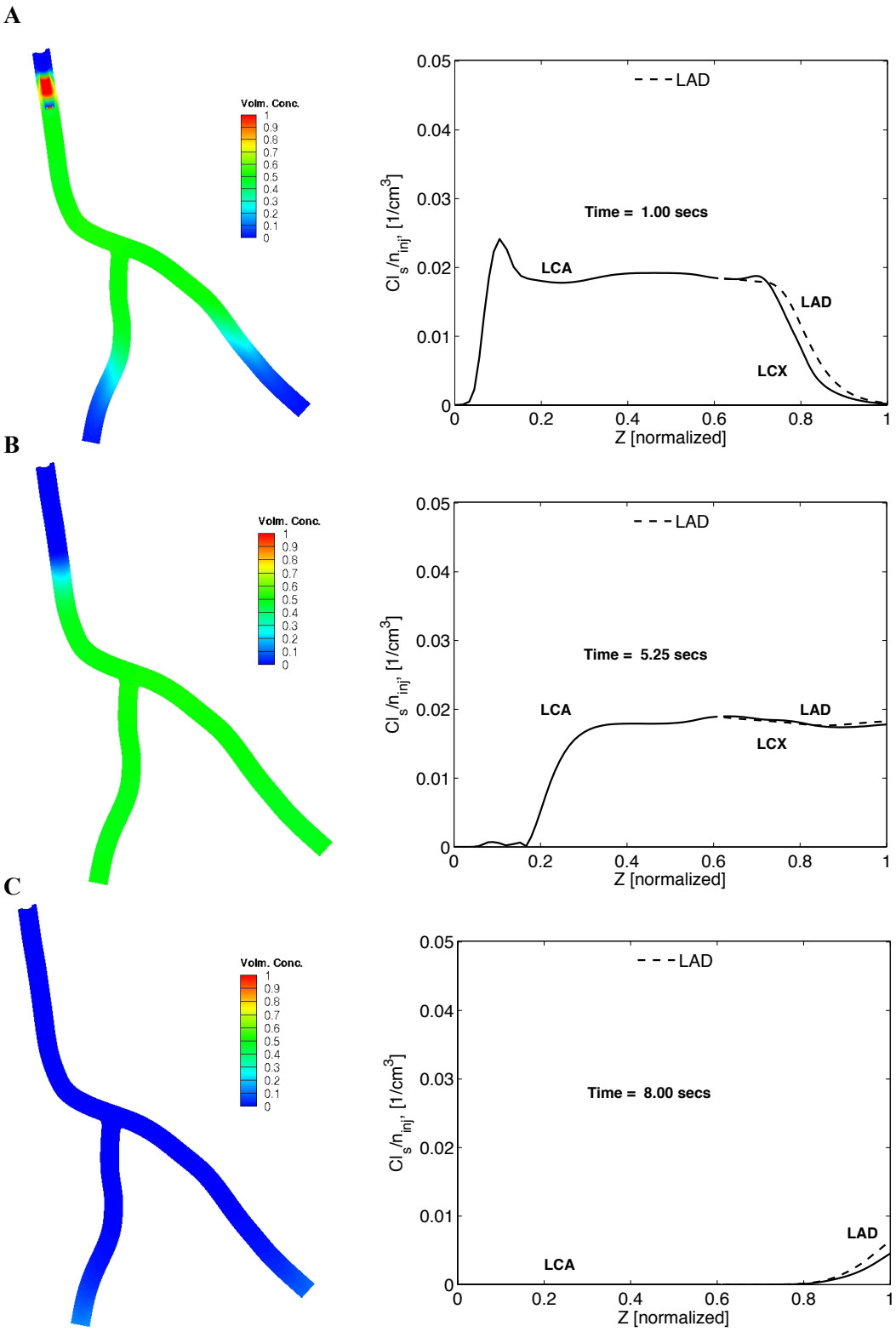

Supplementary Figure 2: Time-integrated particle volumetric concentration (cm^{-3}) $C|_s$ at the lumen-wall interface at the end of simulation (t = 9 s) averaged over the circumference of each cross section taken at various "Z"-locations along the vessel centerline.

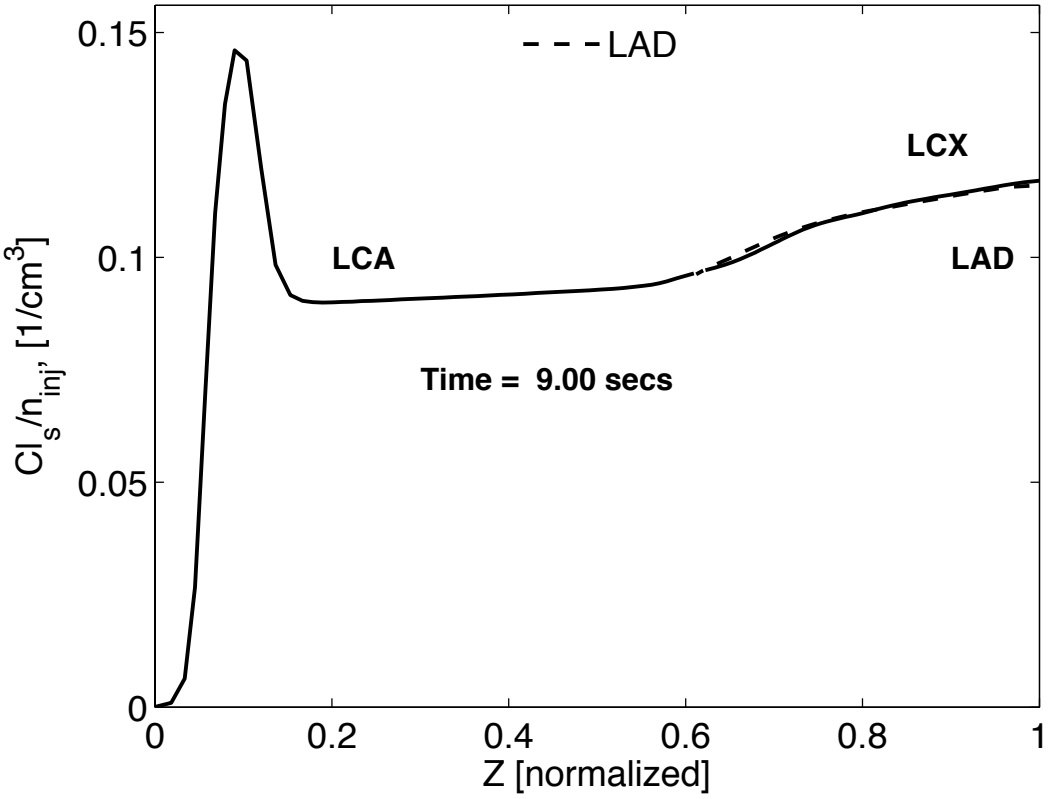

Supplementary Figure 3: Time-averaged wall shear stress (WSS) in Pa (N/m^2) A) during the first 5 s of catheter injection and B) after catheter injection is ceased.

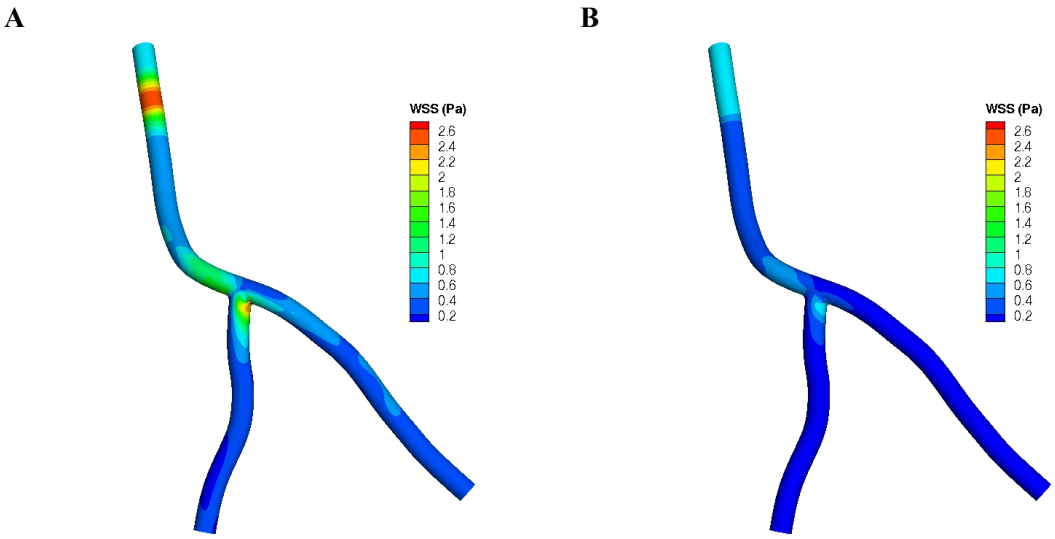

Supplementary Figure 4: Comparison between A) 30:70, B) 50:50, and C) 60:40 aVCAM:aEsel targeting in terms of ($n_{adh}/n_{inj} \times A$), where n_{adh} is the number of adhered particles, n_{inj} is the total number of injected particles, and A is the surface area (cm^2).

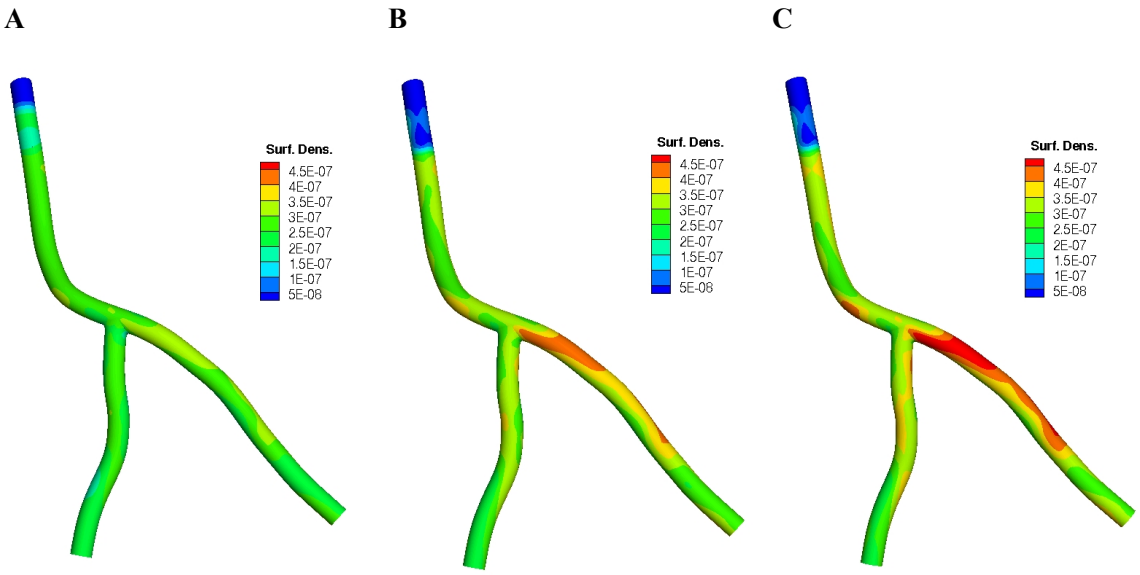

Supplementary Figure 5: Comparison between different proportions of dual targeting. The number of adhering 0.5 μm particles averaged over the circumference of each cross section taken at various "*Z*"-locations along the vessel centerline. Here n_{adh} is the number of adhered particles, n_{inj} is the total number of injected particles, and A is the surface area (cm^2). Comparison between A) 30:70 aVCAM-aEsel, B) 50:50 aVCAM-aEsel and C) 60:40 aVCAM-aEsel cases. Here dashed line represents the LAD branch.

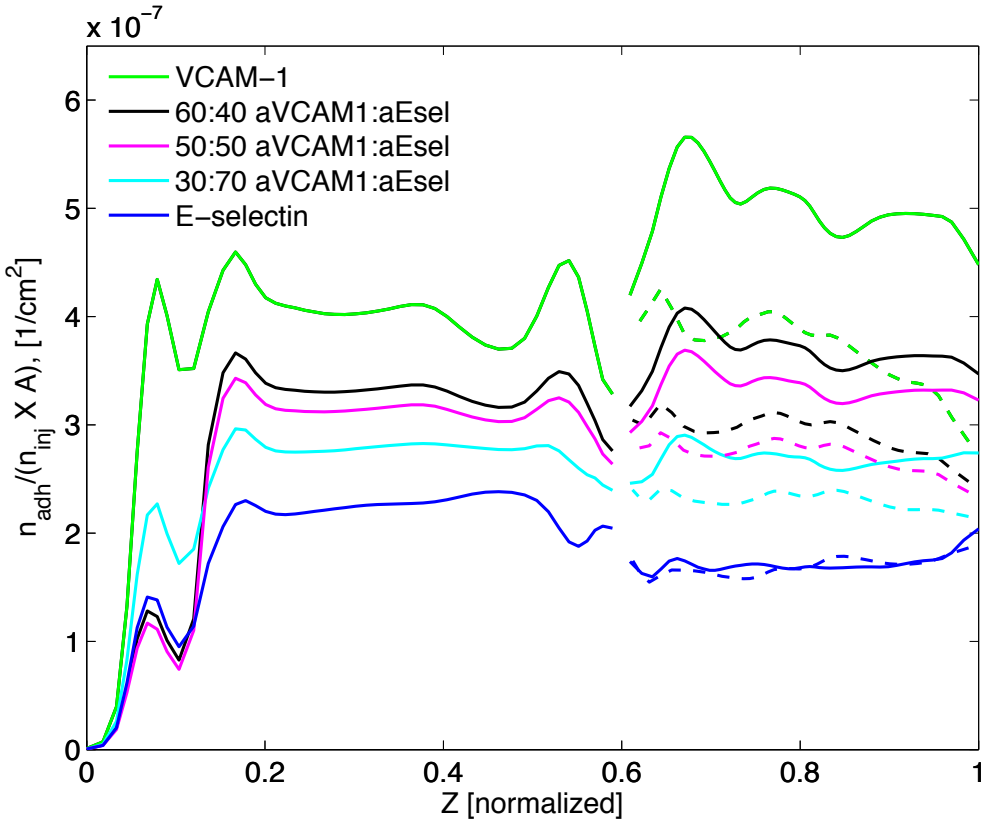

Supplementary Figure 6: Comparison of particle size under single receptor (VCAM-1) targeting. Spatial distribution of different sized particles: A) d_p = 0.1 µm, B) d_p = 0.5 µm and C) d_p = 2.0 µm, in terms of $n_{adh}/(n_{inj} \times A)$, where n_{adh} is the number of adhered particles, n_{inj} is the total number of injected particles and A (cm^2).

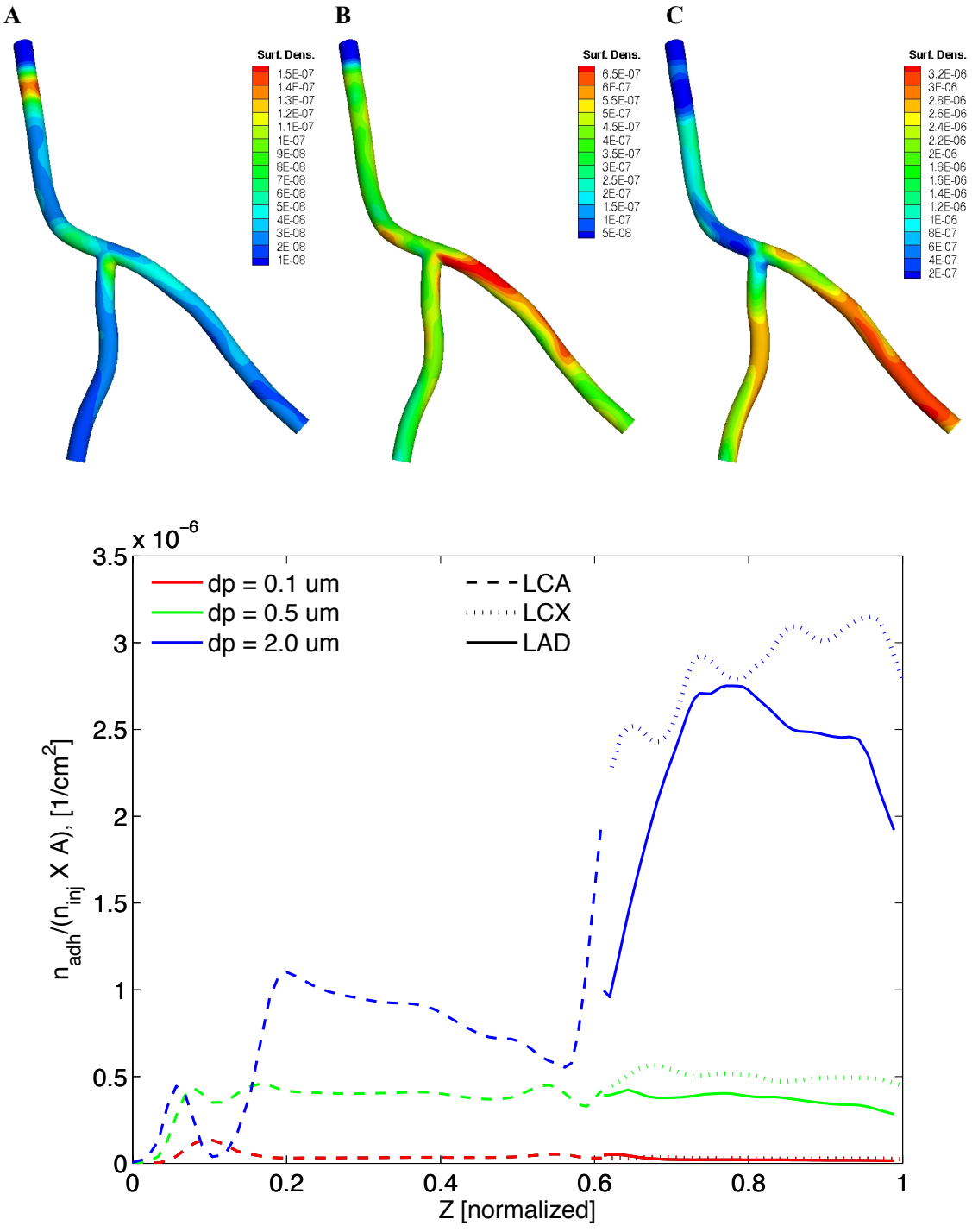

Supplementary Figure 7: Comparison of particle size under single receptor (E-selectin) targeting. Spatial distribution of different sized particles: A) d_p = 0.1 µm, B) d_p = 0.5 µm and C) d_p = 2.0 µm, averaged over the circumference of each cross section taken at various "Z"-locations along the vessel centerline in terms of $n_{adh}/(n_{inj} \times A)$. Here, n_{adh} is the number of adhered particles, n_{inj} is the total number of injected particles and A (cm^2). The dashed line represents the LAD branch.

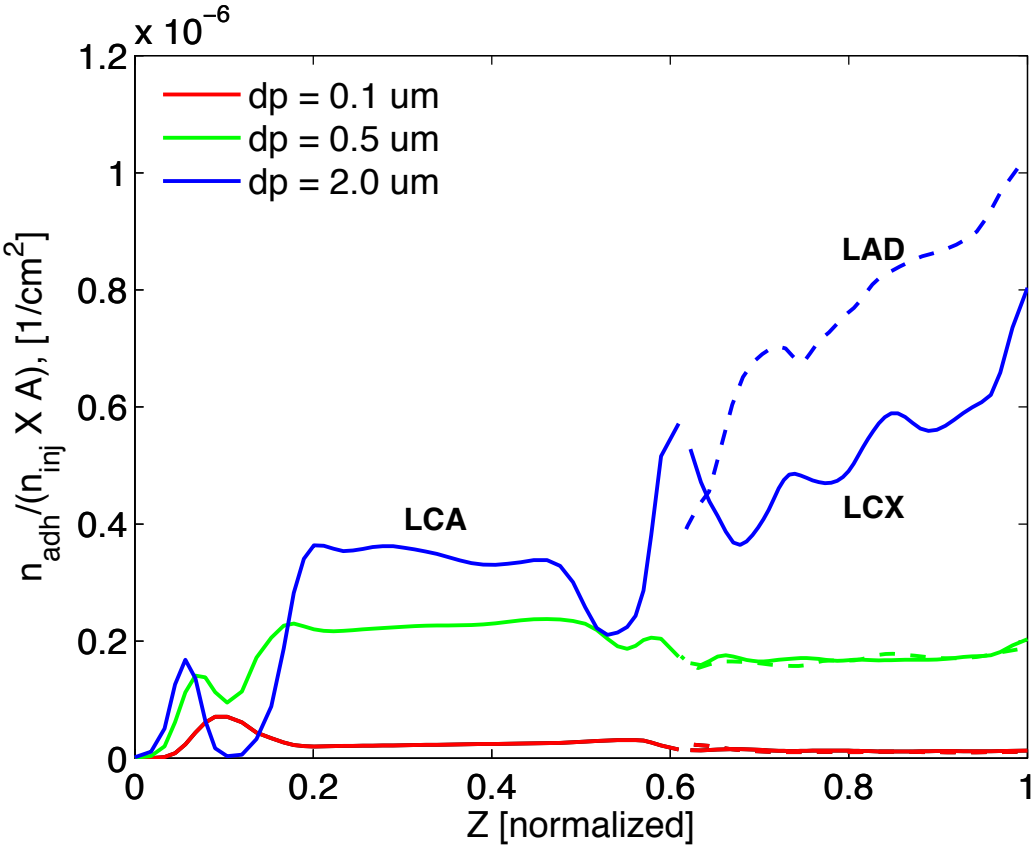

Supplementary Table 1: Area-averaged NP surface density in the arterial tree segment under the single- and dual-targeting approaches.

	Total area-averaged NP surface density, cm^{-2}		
NP type	**Single - receptor targeting approach**		
aICAM-1	7.09×10^{-9}	4.51×10^{-8}	7.48×10^{-8}
aVCAM-1	3.26×10^{-8}	4.14×10^{-7}	1.87×10^{-6}
aEsel	1.82×10^{-8}	1.75×10^{-7}	4.83×10^{-7}
aVCAM-1:aEsel	**Dual - receptor targeting approach**		
30:70	2.25×10^{-8}	2.46×10^{-7}	9.03×10^{-7}
50:50	2.41×10^{-8}	2.86×10^{-7}	1.18×10^{-6}
60:40	2.55×10^{-8}	3.09×10^{-7}	1.32×10^{-6}

Supplementary Table 2: Heterogeneity index, H under the single- and dual-targeting approaches. Here, $H = \frac{N_{LCX}}{N_{LAD}}$, and N is the surface density of particles integrated over the entire surface of the branch and divided by the total surface area of the branch.

	Heterogeneity index, H		
	d_p **= 0.1 µm**	d_p **= 0.5 µm**	d_p **= 2.0 µm**
NP type	**Single-receptor targeting approach**		
aICAM-1	1.06	0.88	0.53
aVCAM-1	1.21	1.35	1.22
aEsel	1.04	1.01	0.70
aVCAM-1:aEsel	**Dual-receptor targeting approach**		
30:70	1.11	1.17	0.99
50:50	1.15	1.23	1.08
60:40	1.16	1.26	1.11